

## Postbuckling Characteristics in Delaminated Kevlar/Epoxy Laminates: An Experimental Study

Authorized Reprint 1990 from Journal of Composites Technology & Research, Summer 1990  
Copyright American Society for Testing and Materials, 1916 Race Street, Philadelphia, PA 19103

**REFERENCE:** Kardomateas, G. A., "Postbuckling Characteristics in Delaminated Kevlar/Epoxy Laminates: An Experimental Study," *Journal of Composites Technology & Research*, JCTRER, Vol. 12, No. 2, Summer 1990, pp. 85-90.

**ABSTRACT:** Compression tests on delaminated kevlar/epoxy specimens were conducted in order to determine the buckling and postbuckling behavior of the system and observe the characteristics of the deformation including growth of the delamination. A broad range of geometric configurations, as far as the location of the delamination through the thickness, was considered. Both the initiation resistance, defined as the applied displacement per specimen length and the growth resistance, defined as the applied displacement per unit delamination growth during the postbuckling stage were quantified for each configuration. For the particular case studied, it was found that the growth resistance is infinite (that is, no growth) for delamination thickness/total thickness ratio  $H/T = 1/15$ , becoming 0.52 for  $H/T = 2/15$  and dropping to a value of only 0.07 for  $H/T = 4/15$ . The initiation resistance is also lowered as the delamination is located further away from the specimen surface and for  $H/T = 4/15$  growth initiation occurred before peak load. The experimental program investigates also the development of the deformation regarding the postbuckled shape, the load-displacement curve and the corresponding growth of the delamination. Furthermore, a comparison with analytical solutions for the postbuckling behavior at large applied displacements is performed.

**KEYWORDS:** composites, delamination, buckling, postbuckling, tests, growth rate, compression, kevlar/epoxy

For structures that are required to maintain their integrity despite the presence of defects, it is important to be able to predict their macroscopic behavior in presence of these defects and understand the conditions for growth of the defects and how such growth would affect the load carrying capacity. In composites, delaminations are a common defect arising from service loads or manufacturing imperfections.

The work on the subject of delamination buckling has been focused to date mainly on formulating analytical solutions for the prediction of the buckling load and the initial postbuckling behavior [1-4]. Few experimental studies have been reported especially on the growth of the delamination and the macroscopic behavior during continuing postbuckling deflections. In Ref 5 the experiments were performed on a random short-fiber SMC-R50 composite, and the study was focused on the buckling stress. In Ref 6, the study was focused on the postbuckling behavior at large applied displacements, and some experimental results on the macroscopic behavior for thin delaminations were reported.

<sup>1</sup>Assistant professor, School of Aerospace Engineering, Georgia Institute of Technology, Atlanta, GA 30332-0150.

In general, whether growth of the delamination takes place or not, depends on the geometric configuration (location and extent of the delamination), the material and the loading history. The postbuckling deflections impose a history of stress, strain, and rotation at the delamination tip corresponding to the load-deflection history. Questions of importance are determining the initiation of growth point (a relevant issue of interest is, for example, if growth starts before peak load), the growth rate (that is, delamination growth per unit applied deflection) and the corresponding load levels. Indirectly, these measures are useful in considering such concepts as the compliance of the system since lower values of growth resistance would indicate reduced specimen stiffness. The above constitutes the objectives of the present paper, that is, a detailed experimental study and interpretation of the behavior of delaminations during the postbuckling stage.

### Experimental Study

#### Material and Experimental Procedure

The material used in the experimental study was unidirectional prepreg Kevlar 49 of the following specifications: commercial type SP-328, nominal thickness per ply 0.20 mm (0.008 in.), nominal stiffness  $E_1 = 75.8 \text{ GN/m}^2$  ( $11 \times 10^6$  psi),  $E_2 = 5.5 \text{ GN/m}^2$  ( $0.8 \times 10^6$  psi),  $G_{12} = 2.1 \text{ GN/m}^2$  ( $0.3 \times 10^6$  psi), Poisson's ratio  $\nu_{12} = 0.34$ , where 1 is the direction along the fibers. A delamination of length  $l = 2a = 50.8 \text{ mm}$  (2 in.) was introduced by a 0.025-mm (0.001-in.) thick Teflon® strip placed in the middle of the length between the plies and through the width. The length between the grips for the specimens was  $L = 101.6 \text{ mm}$  (4 in.). A width of  $W = 12.7 \text{ mm}$  (0.5 in.) was used to keep the load level small and prevent any possible bending of the grips. The material was cured at 250°F (120°C) and 80 psi for 2 h followed by an 8 h cooling cycle to room temperature and pressure. Since the curing process affects the final dimensions, the exact thickness for the specimen was measured (with a micrometer) after curing. It was found to be  $T = 3.81 \text{ mm}$  (0.150 in.). In addition, the exact axial modulus was also measured after curing from a simple tension test on strain gauged coupons, and it was found to be  $E_1 = 68.2 \text{ GN/m}^2$  ( $9.9 \times 10^6$  psi). The tests were conducted in a 20-kip (89-kN) MTS servo-hydraulic machine. They were carried out on stroke control with a rate of about 0.8 mm/min. The specimen was clamped at the upper grip and a special fixture at the lower grip. The latter one was designed so that the specimen slides into it and therefore no bending is introduced by tightening the end. To be able to com-

pare with any theoretical model, the compliance of the testing machine is also needed. It was measured from a simple compression test (without a specimen) and was found to be  $0.685 \times 10^{-4}$  mm/N ( $0.12 \times 10^{-4}$  in/lb.). To be able to measure possible growth of the delamination, measuring tape was put at both ends of the specimen.

#### Discussion of Test Results

Let us observe the deformation history for some specimen configurations by considering the load versus displacement curves and pictures of the specimen shape at certain instances. Figures 1 and 2 refer to the case of a delamination between first and second ply, in a 15-ply specimen, that is, the case of  $H/T = 1/15$ . In Fig. 1 the first arrow corresponds to the first observation of the delaminated layer buckling out while the second arrow points to the specimen picture at peak load (applied displacement  $\delta = 0.05$  in. [1.27 mm]). In Fig. 2 the postbuckled shape is shown during the dropping load phase of the load-deflection curve. It

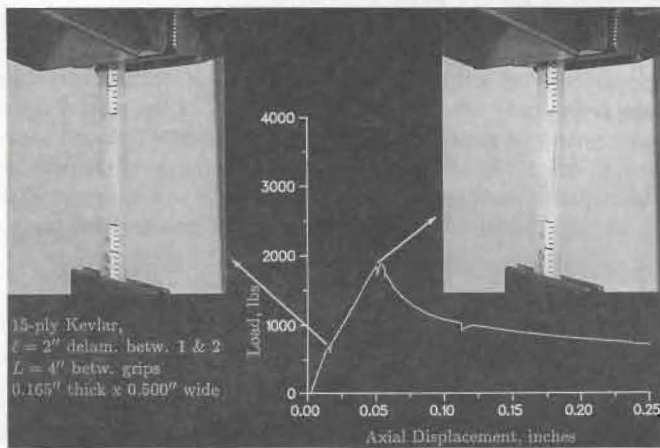


FIG. 1—The postbuckled shape at the initial postbuckling stage (increasing load) for  $H/T = 1/15$ .

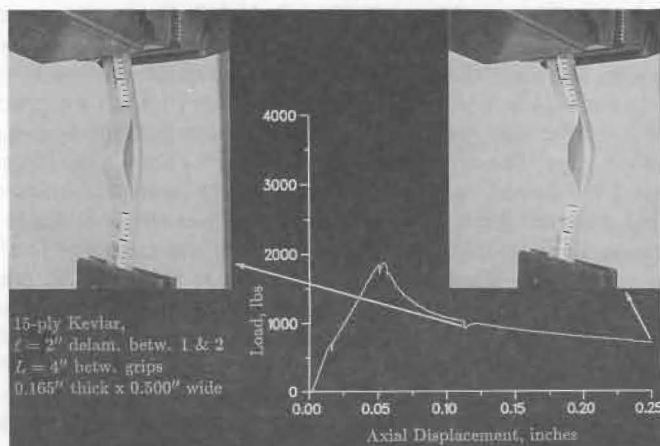


FIG. 2—The postbuckled shape during continuing postbuckling deformation (phase of decreasing load) for  $H/T = 1/15$ . No growth of the delamination is seen.

should be noted that the theory in Ref 6 would predict a load peaking out; however a dropping load cannot be predicted from an ideal postbuckling analysis, and we need to couple this with a damage model to be able to account for the load drop. Although in Fig. 2 the applied displacement was increased up to  $\delta = 0.25$  in. (6.35 mm), we could see *no growth* of the delamination. It should be noted that a load versus displacement curve of a virgin specimen (that is, with no Teflon® implant) in comparison with the behavior of the specimen with an implant has been provided in Ref 6.

Figures 3 and 4 show the deformation history for a specimen configuration of  $H/T = 3/15$ , that is, the delamination was between third and fourth ply in a 15-ply construction. In Fig. 3 the first arrow shows the point where buckling out of the delaminated layer becomes visible (rising load and at applied displacement  $\delta = 0.02$  in. [0.58 mm]) whereas the second arrow corresponds to the postbuckled shape at peak load (applied displacement  $\delta = 0.03$  in. [0.762 mm]). No growth is seen as yet. In Fig. 4 two points beyond peak load are shown; at the first point (applied

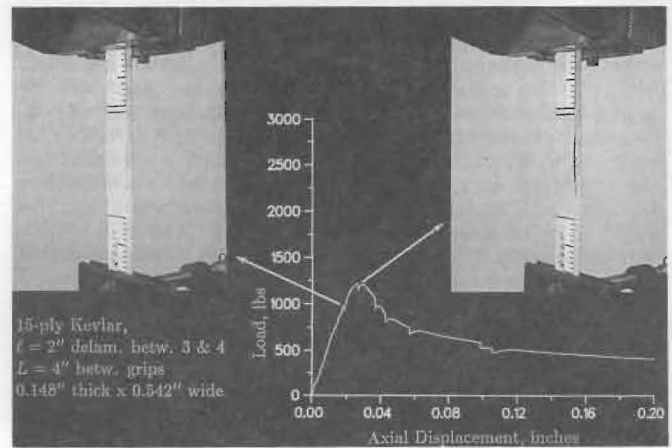


FIG. 3—The postbuckled shape at the initial postbuckling stage (increasing load) for  $H/T = 3/15$ .

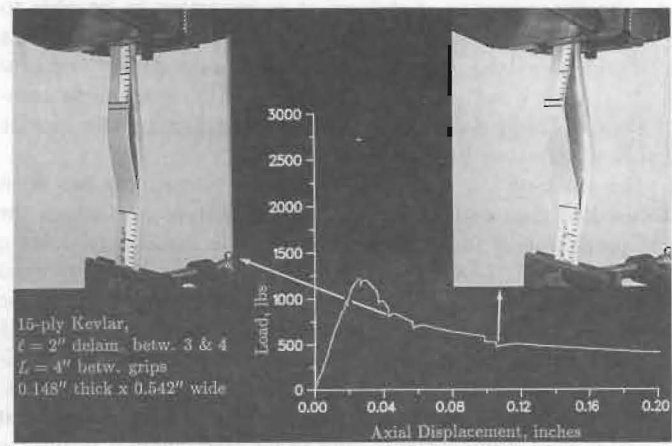


FIG. 4—The postbuckled shape during continuing postbuckling deformation (phase of decreasing load) for  $H/T = 3/15$ . The delamination has grown up to the grip at the upper side and by about 0.25 in. (63.5 mm) at the lower side at applied displacement of 0.11 in. (28 mm).

displacement  $\delta = 0.04$  in. [1.016 mm]) the delamination has grown towards the upper grip by about 0.5 in. (12.7 mm) whereas at the second point (applied displacement  $\delta = 0.11$  in. [2.79 mm]) the delamination has grown up to the grip at the upper end and by about 0.25 in. (6.35 mm) at the lower end. This behavior is in contrast to the behavior of the specimen with  $H/T = 1/15$  where no growth was seen at all. We continued applying the deformation, and in Fig. 5 it is seen that the delamination has grown for 0.5 in. (12.7 mm) towards the lower grip (in addition to having grown on the entire ligament towards the upper grip) at applied displacement  $\delta = 0.25$  in. (6.35 mm); it has grown on the entire ligament towards the lower grip for applied displacement  $\delta = 0.5$  in. (6.35 mm).

Next, the case of  $H/T = 4/15$  is shown in Figs. 6 and 7. In Fig. 6, it is seen that growth towards the upper grip has already started before peak load, and the delamination has grown up to the grip at the upper side of  $\delta = 0.05$  in. (1.27 mm). In Fig. 7

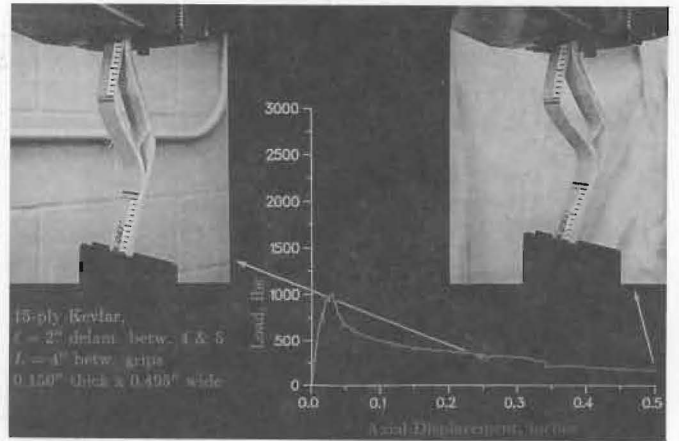


FIG. 7—The postbuckled shape during continuing postbuckling deformation for  $H/T = 4/15$ . The deformation is focused on the upper side whereas the delamination on the lower side is closing.

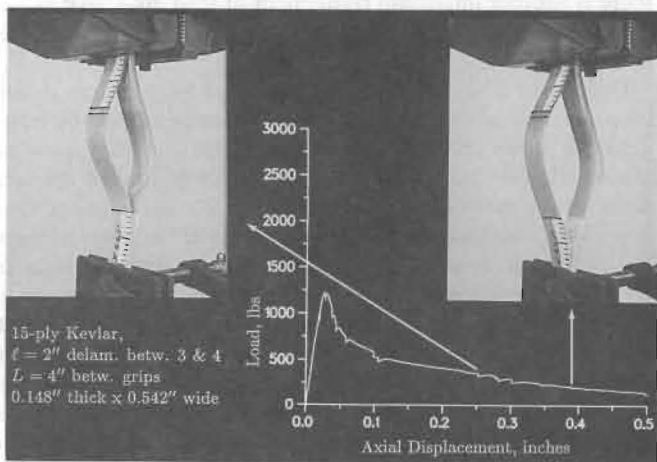


FIG. 5—The postbuckled shape during continuing postbuckling deformation (phase of decreasing load) for  $H/T = 3/15$ . The delamination has grown on the entire ligament towards both grips at applied displacement of 0.5 in. (12.7 mm).

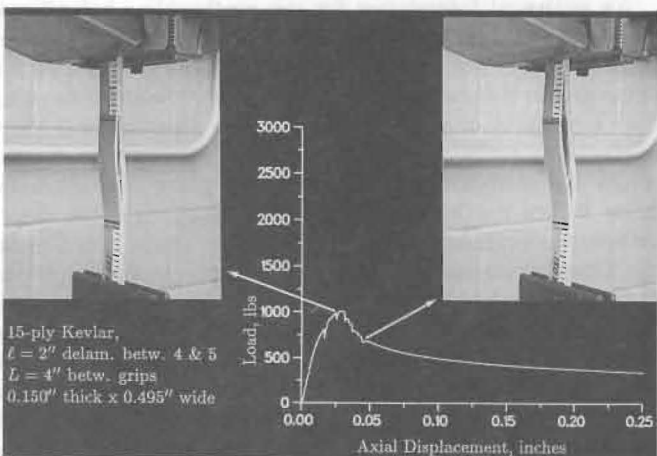


FIG. 6—The postbuckled shape at the initial postbuckling stage for  $H/T = 4/15$ . Growth starts before peak load.

the applied displacement was increased further, and it is seen that the buckling deflections become focused on the upper part whereas the delamination at the lower part is closing (instead of observing growth towards the lower grips as in Fig. 4). The asymmetric behavior as regards the upper and lower sides of the specimen was observed in several specimens, and it is due to the lack of perfect symmetry in the end fixing of the specimen. In many specimens, on the other hand, the growth took place towards both grips at the same time. However, the existence of asymmetries in end fixity is quite natural and most often encountered in practice.

From the above it is clear that the postbuckling behavior as regards the growth of the delamination and the postbuckled shape of the system is quite different for different geometric configurations and depends directly on the location of the delamination through the thickness. First we need to define the initiation point and obtain a measure of the initiation resistance for the configurations studied. Table 1 shows the initiation resistance quantified as the applied displacement (normalized with respect to the specimen length) required for initiation of growth,  $\delta/L$ . For the case of  $H/T = 1/15$  no growth was seen, therefore the resistance to initiation is infinite, whereas the initiation resistance  $\delta/L$  has a value of 0.020 for  $H/T = 2/15$  and becomes only 0.006 for  $H/T = 4/15$ . Table 2 summarizes the growth resistance for the cases that were investigated in this experimental program. The delamination growth resistance  $R_g$  is quantified here by the applied displacement required per unit delamination growth (that is averaged for the entire test)

$$R_g = \Delta\delta/\Delta a$$

TABLE 1—Initiation displacement.

Delamination $H/T$	Initiation Displacement $\delta/L$
1/15	$\infty$
2/15	0.020
3/15	0.009
4/15	0.006

TABLE 2—Delamination growth resistance.

Delamination location $H/T$	Growth Resistance $\Delta\delta/\Delta\alpha$
SYMMETRIC GROWTH TESTS (SIMULTANEOUS GROWTH TOWARDS BOTH GRIPS)	
1/15	$\infty$
2/15	0.52
3/15	0.20
4/15	0.07
ASYMMETRIC GROWTH TESTS (GROWTH TOWARDS THE ONE GRIP ONLY)	
1/15	$\infty$
2/15	0.23
3/15	0.06
4/15	0.02

Since there were two kinds of observed growth, one in which the delamination grew at the same time symmetrically towards both ends from the beginning, and another where growth occurred initially towards one end only, we calculated the growth resistances for both cases in Table 2. It is seen that the growth resistance is decreasing for delaminations located further away from the surface. Thus the growth resistance  $R_g$  for the tests with symmetric growth is 0.52 for  $H/T = 2/15$  and becomes only 0.07 for  $H/T = 4/15$ . For the tests with asymmetric growth (growth focused on one end of the specimen) the resistance is even smaller.

Although the definitions that quantify the initiation and growth resistance are somewhat empirical, they offer the advantage of being easily measured and therefore can give readily an overall description of the behavior. It should also be noted that growth of the delamination generally takes place in spurts or steps and for a more accurate description of the behavior, the amount of the stable growth and the rate of growth at each step would be needed. The present work is looking at an overall description of the growth phase. Since the buckling deflections are included in the definition of  $R_g$ , this quantity relates the applied displacement with delamination growth as opposed to a fracture mechanics quantity that would connect near tip quantities. Moreover, the quantity defined above  $R_g$  is useful because it can be approximately related to the load drop. The total applied load is that from the buckling of the upper part and that from the buckling of the lower part of the specimen. Assume that the load during postbuckling does not change appreciably from the buckling load, then the total applied load is

$$P = \frac{E_1 W H^3}{12(1 - \nu_{13}\nu_{31})} \frac{\pi^2}{a^2} + \frac{E W (T - H)^3}{12(1 - \nu_{13}\nu_{31})} \frac{\pi^2}{a^2}$$

where  $l = 2a$  is the delamination length,  $W$  is the width of the specimen,  $H$  and  $T$  are the thicknesses of the delaminated layer and the specimen, and  $\nu_{13}$ ,  $\nu_{31}$  are Poisson's ratio's. Notice that it has already been observed [6] that the load does not remain constant during postbuckling but it drops (for example, one reason is the accumulated damage). It is, therefore, understood that the above expression is only an approximation used to derive a simple expression. Based on this approximation, for growth through the ligament,  $L - l$ , the change in load corresponds to

the difference in the buckling loads for the upper and lower parts of initial length  $l$  (delamination length) and final length  $L$  (specimen length, for complete growth)

$$\Delta P = \frac{4\pi^2 E_1 W}{12(1 - \nu_{13}\nu_{31})} [T^3 - 3TH(T - H)] \left( \frac{1}{l^2} - \frac{1}{L^2} \right)$$

Therefore, the delamination growth is reflected on a reduction in stiffness, and the load drop per unit applied displacement would be approximately given by

$$\Delta P/\Delta\delta = \frac{\Delta P}{\Delta a} \frac{\Delta a}{\Delta\delta} = \frac{4\pi^2 E_1 W}{12(L - l)(1 - \nu_{13}\nu_{31})} \times [T^3 - 3TH](T - H) \left( \frac{1}{l^2} - \frac{1}{L^2} \right) \frac{1}{R_g}$$

The falling part of the load displacement curve was indeed steeper for the cases of higher growth rate (low  $R_g$ ); however there is another important component of load drop, that caused by damage accumulation, and this subject is still not well understood.

Of interest is also the strain experienced by the upper delaminated layer and the lower part during the postbuckling stage. Figure 8 shows both the strain at the middle of the upper delaminated layer and the load as a function of applied displacement for the case of  $H/T = 2/15$ . Initially the delaminated layer is uniformly compressed (negative strain); at the point of buckling the strain reverses sign and continues to increase at an increasing rate until peak load and subsequently continues to increase at a decreasing rate. Figure 9 shows the strain at the middle of the lower part for  $H/T = 3/15$ . Transverse deflections of the lower part are important in determining the behavior of the whole system [6]. Again, the lower part is uniformly compressed in the beginning (negative strain) until bending deformation is induced at which point the strain becomes tensile. This occurs a little before peak load. The strain is seen then to increase at a decreasing rate.

#### Comparison with Analytical Predictions

An analytical formulation for the postbuckling behavior of composites including the effects of large deflections of the delaminated layer was presented in Ref 6. In this formulation the deformation of the delaminated layer was represented by using the exact theory of plane deformation of a prismatic bar, which is elastically restrained at the ends by means of concentrated forces and moments; for the rest of the plate, the cylindrical beam theory was used. For the delaminated layer the deformation was expressed in terms of two generalized coordinates: the distortion parameter  $\alpha$ , which is the angle of tangent rotation at the inflection point from the straight position, and the end-amplitude variable  $\Phi_e$ . The analysis predicted the load peaking out; the load drop observed during the subsequent (beyond peak load) applied displacements in the tests described above is due to the induced damage. Figure 10 shows a comparison of the strain at the middle of the delaminated layer with the theoretical predictions from the large deflections model of Ref 6 for the case of  $H/T = 1/15$ . This theoretical strain is given in terms of

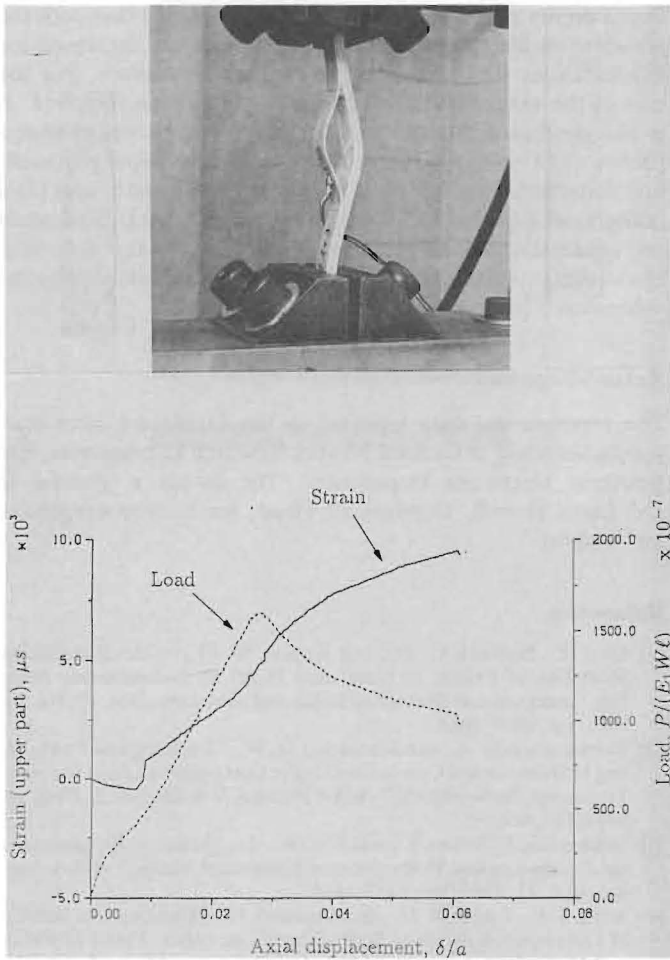


FIG. 8—Strain at the middle of the upper delaminated layer and corresponding load versus applied displacement for  $H/T = 2/15$ . The point of sign reversal for the strain is the point of buckling for the delaminated layer. In the upper picture the strain gage location is shown.

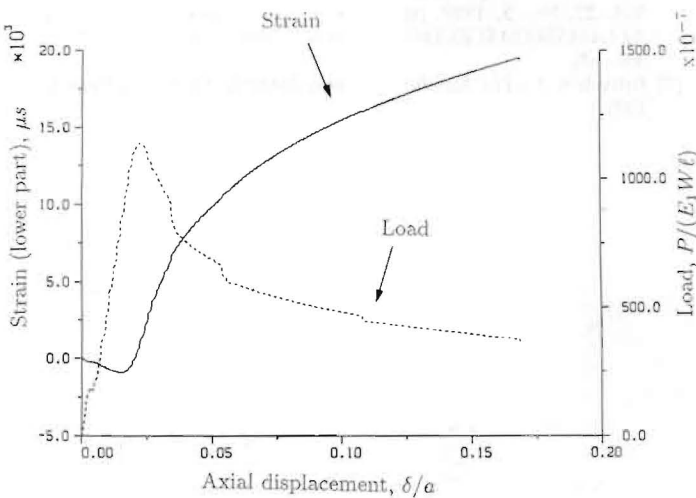


FIG. 9—Strain at the middle of the lower part and corresponding load versus applied displacement for  $H/T = 3/15$ . Transverse deflections (tensile strains) are induced in the lower part a little before peak load.

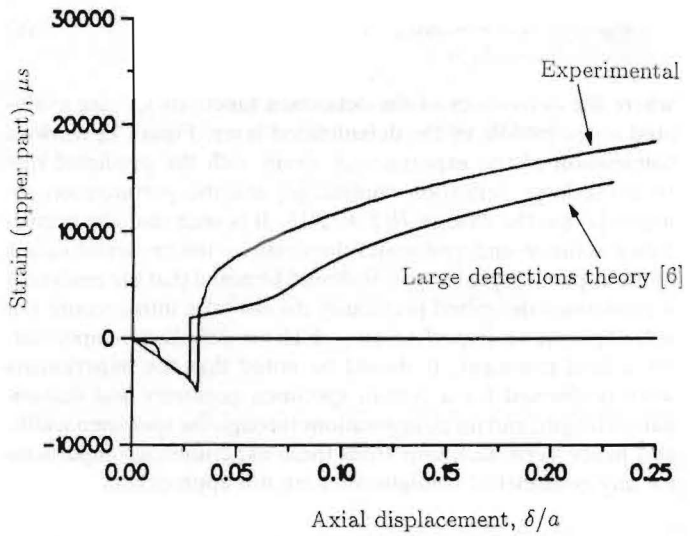


FIG. 10—Comparison of theory with experiments on the strain at the middle of the upper delaminated layer for  $H/T = 1/15$ .

the radius of curvature  $\rho$  at the middle of the delaminated layer and the thickness of the layer  $H$  as follows

$$\epsilon_u = H/(2\rho) \tag{1}$$

From Britvek [7] and Ref 6, the curvature is found

$$\frac{1}{\rho} = \frac{4k}{l} F_u \tag{2}$$

where

$$k = k(\alpha) = \sin(\alpha/2) \tag{3}$$

and

$$F_u = F_u(\alpha, \Phi_u) = \int_0^{\Phi_u} \frac{d\phi}{\sqrt{1 - k^2 \sin^2 \phi}} \tag{4}$$

Therefore, by substituting Eq 2 in Eq 1, we obtain the following expression for the strain

$$\epsilon_u = \epsilon_u(\alpha, \Phi_u) = \frac{2Hk}{l} F_u \tag{5}$$

Notice that the generalized coordinates of deformation  $\alpha$  and  $\Phi_u$  are known at each stage of postbuckling deformation and the corresponding applied load and displacement are also given in terms of these variables [6].

In Ref 2 a perturbation solution for the initial postbuckling behavior was developed. The solution was based on developing the deflection and load quantities of each constituent part into ascending perturbation series with respect to the angle at the common section  $\phi$ . For this solution, the strain at the upper part would be given again from Eq 1 where now

$$\frac{l}{\rho} = \phi y_{u,1}'' + \phi^2 y_{u,2}'' + \dots \quad (6)$$

where the derivatives of the deflection functions  $y_{u,i}''$  are evaluated at the middle of the delaminated layer. Figure 11 shows a comparison of the experimental strain with the predicted one from the large deflection analysis [6] and the perturbation solution [2] for the case of  $H/T = 2/15$ . It is seen that the perturbation solution underestimates the strain for the moderate values of the applied displacement. It should be noted that the analytical formulations described previously do not take into account the role of geometric imperfections, which nevertheless is important. As a final comment, it should be noted that the experiments were performed for a certain specimen geometry and delamination length, and for delaminations through the specimen width, and hence generalizations from these experiments/comparisons for any geometrical configuration are not appropriate.

### Concluding Comments

The characteristics of the postbuckling deformation in delaminated kevlar/epoxy specimens were studied in an experimental program that includes different geometric configurations. The

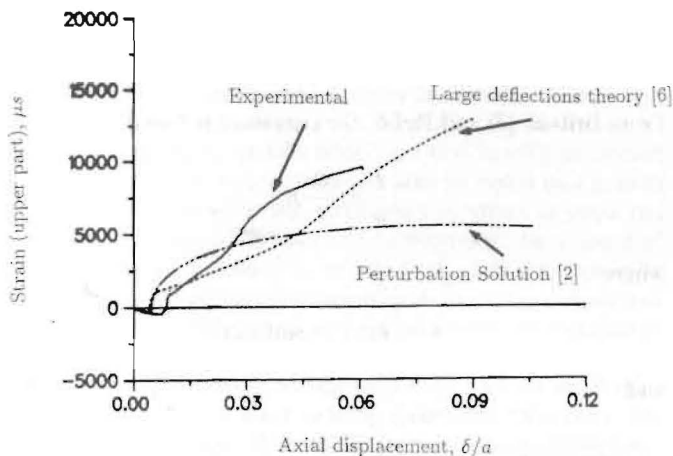


FIG. 11—Comparison of the experimental strain at the middle of the upper delaminated layer with the theoretical predictions for  $H/T = 2/15$ .

study focuses on quantifying the delamination growth resistance. Based on the experimental results, it is concluded that both the initiation displacement and the growth rate are increased for delaminations located further away from the surface. For the case of the very thin delamination, no growth was observed. It is also concluded that the load deflection curves consist of two phases: (1) a rising load stage that includes the initial postbuckling deflections, and for most cases is free of growth, and (2) a falling load stage that includes mostly growth of the delamination and accumulated damage. A comparison of the test data with theoretical predictions on the levels of strain experienced by the delaminated layer is performed.

### Acknowledgement

The experimental data reported in this article are from tests conducted while at General Motors Research Laboratories, Engineering Mechanics Department. The author is grateful to Dr. Larry Howell, Department Head, for his encouragement and support.

### References

- [1] Chai H., Babcock C. D., and Knauss W. G., "One Dimensional Modelling of Failure in Laminated Plates by Delamination Buckling," *International Journal of Solids and Structures*, Vol. 17, No. 11, 1981, pp. 1069-1083.
- [2] Kardomateas G. A. and Schmueser D. W., "Buckling and Postbuckling of Delaminated Composites Under Compressive Loads Including Transverse Shear Effects," *AIAA Journal*, Vol. 26, No. 3, 1988, pp. 337-343.
- [3] Simitzes G. J., Sallam S., and Yin, W. -L., "Effect of Delamination on Axially-Loaded Homogeneous Laminated Plates," *AIAA Journal*, Vol. 23, 1985, pp. 1437-1444.
- [4] Wang S. S., Zahlan N. M., and Suemasu, H., "Compressive Stability of Delaminated Random Short-Fiber Composites, Part I-Modeling and Methods of Analysis," *Journal of Composite Materials*, Vol. 19, 1985, pp. 296-316.
- [5] Wang S. S., Zahlan N. M., and Suemasu H., "Compressive Stability of Delaminated Random Short-Fiber Composites, Part II-Experimental and Analytical Results," *Journal of Composite Materials*, Vol. 19, 1985, pp. 317-333.
- [6] Kardomateas G. A., "Large Deformation Effects in the Postbuckling Behavior of Composites With Thin Delaminations," *AIAA Journal*, Vol. 27, No. 5, 1989, pp. 624-631; also, *Proceedings, 29th SDM AIAA/ASME/ASCE/AHS Conference*, Williamsburg, VA, 1988, pp. 382-390.
- [7] Britvek S. J., *The Stability of Elastic Systems*, Pergamon Press Inc., 1973.